

Electronic supplementary information

Identifying the best metal–organic frameworks and unravelling different mechanisms for the separation of pentane isomers

Zhiwei Qiao,^{ab} Anthony K. Cheetham^{cd} and Jianwen Jiang^{*a}

^a*Department of Chemical and Biomolecular Engineering, National University of Singapore, 117576, Singapore*

^b*School of Chemistry and Chemical Engineering, Guangzhou University, Guangzhou 510006, China*

^c*Department of Materials Science and Engineering, National University of Singapore, 117576, Singapore*

^d*Materials Research Laboratory, University of California, Santa Barbara, CA 93106, USA*

Table of Contents

1. Physical properties of C ₅ isomers	S2
2. Adsorption energies of single C ₅ isomers	S2
3. VICDOC	S3
4. Best MOFs with six separation mechanisms	S4
5. Adsorption capacity and selectivity <i>versus</i> ϕ , LCD and VSA	S5
6. Pore size distribution between d_1 and d_2	S6
7. Simulation snapshots for different separation mechanisms	S7
8. Molecular models	S13

1. Physical properties of C₅ isomers

Table S1 Physical properties of C₅ isomers.¹

Isomer	Boiling point (°C)	Critical temperature (°C)	Critical pressure (bar)	Kinetic diameter (Å)
<i>n</i> -C ₅	36.0	196.6	33.6	4.3
<i>iso</i> -C ₅	27.7	187.8	33.8	5.0
<i>neo</i> -C ₅	9.5	160.6	31.9	6.2

2. Adsorption energies of single C₅ isomers

Table S2 Adsorption energies of single C₅ isomers in MOFs with very large pores.

MOF	PLD (Å)	LCD (Å)	ΔE (kJ/mol)		
			<i>n</i> -C ₅	<i>iso</i> -C ₅	<i>neo</i> -C ₅
BAZGAM	24.24	42.80	-18.61	-17.66	-15.64
BEDYEQ	31.49	33.06	-32.29	-30.48	-27.81
RAVXIX	56.26	53.58	-36.46	-35.06	-31.43
RAVXOD	71.50	71.64	-36.99	-34.91	-30.25

3. VICDOC

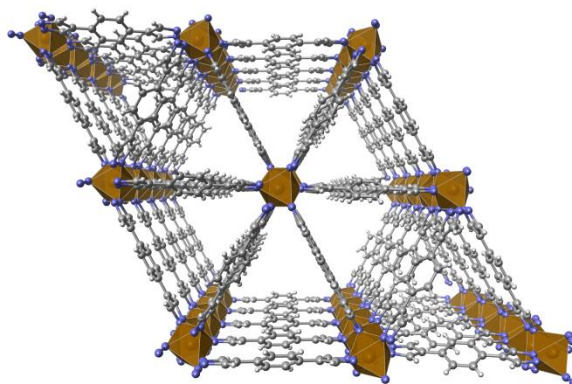


Fig. S1 VICDOC.

Table S3 Adsorption of equimolar C₅ isomer mixture in VICDOC at 373 K and a total pressure of 30 kPa.

N_{C_5} (mol/kg)	2.59
N_{n-C_5} (mol/kg)	2.48
N_{iso-C_5} (mol/kg)	0.11
N_{neo-C_5} (mol/kg)	4.20×10^{-5}
$S_{n-iso-C_5}$	22.97
$S_{n-neo-C_5}$	5.91×10^4
$S_{iso-neo-C_5}$	2.57×10^3

4. Best MOFs

Table S4 Best MOFs with six separation mechanisms.

Type	Separation*	Benchmark	CSD code	LCD (Å)	N_{C_5} (mol/kg)	$S_{n-/iso-C_5}$ [$S_{iso-/n-C_5}$]**	$S_{n-/neo-C_5}$ [$S_{neo-/n-C_5}$]**	$S_{iso-/neo-C_5}$ [$S_{neo-/iso-C_5}$]**
1	<i>n-/iso-C₅</i> <i>n-/neo-C₅</i>	$N_{C_5} > 1$ mol/kg $S_{n-/iso-C_5} > 6000$ $S_{n-/neo-C_5} > 10^4$	ADIQEL	4.43	2.75 ± 0.04	$(8.18 \pm 0.69) \times 10^4$	$> 10^6$	
			WUCRUH	4.32	1.13 ± 0.06	$(6.08 \pm 1.42) \times 10^3$	$> 10^6$	
			HEXNII	4.82	1.17 ± 0.02	$(1.50 \pm 0.77) \times 10^4$	$> 10^6$	
			MIMVEJ	4.72	2.32 ± 0.05	$(9.18 \pm 2.85) \times 10^5$	$> 10^6$	
			FUDQIF	4.38	1.32 ± 0.06	$> 10^6$	$> 10^6$	
			PARMIG	4.62	2.20 ± 0.11	$> 10^6$	$> 10^6$	
2	2i <i>n-/neo-C₅</i> <i>iso-/neo-C₅</i>	$N_{C_5} > 1.9$ mol/kg $N_{iso-C_5} > 0.4$ mol/kg $S_{n-/neo-C_5} > 400$ $S_{iso-/neo-C_5} > 400$	XUNGOD	5.28	2.31 ± 0.26		$(4.88 \pm 0.78) \times 10^2$	$(4.22 \pm 0.71) \times 10^2$
			GIFKAH	4.61	1.92 ± 0.33		$> 10^6$	$> 10^6$
			AFITEP	4.64	2.63 ± 0.36		$> 10^6$	$> 10^6$
			2ii <i>n-/neo-C₅</i> <i>iso-/neo-C₅</i>	$N_{C_5} > 1.9$ mol/kg $N_{iso-C_5} > 0.4$ mol/kg $S_{n-/neo-C_5} > 400$ $S_{iso-/neo-C_5} > 400$	GOGWAB	4.96	2.82 ± 0.59	
WAZQIZ	5.13	2.15 ± 0.32			$(2.10 \pm 0.40) \times 10^3$	$(1.15 \pm 0.28) \times 10^3$		
3	3i <i>iso-/n-C₅</i> <i>neo-/n-C₅</i>	$N_{C_5} > 0.4$ mol/kg $S_{iso-/n-C_5} > 8$ $S_{neo-/n-C_5} > 10$	INAMUG	5.66	0.89 ± 0.22	0.091 ± 0.077 [11.05 ± 9.43]	0.032 ± 0.023 [31.50 ± 23.27]	
			XUVGUQ	5.67	0.43 ± 0.09	0.053 ± 0.017 [18.78 ± 6.05]	0.032 ± 0.008 [31.18 ± 7.65]	
			MAJHUC	5.75	0.91 ± 0.29	0.119 ± 0.058 [8.38 ± 4.09]	0.088 ± 0.021 [11.32 ± 2.72]	
			OVICUS	5.89	1.26 ± 0.22	0.044 ± 0.026 [22.71 ± 13.43]	0.037 ± 0.022 [26.99 ± 15.79]	
			SEMFIB	6.30	1.98 ± 0.37	0.094 ± 0.068 [10.59 ± 7.60]	0.031 ± 0.020 [31.84 ± 20.48]	
			SEMFEX	5.92	2.14 ± 0.27	0.063 ± 0.015 [15.88 ± 3.89]	0.024 ± 0.003 [41.14 ± 5.42]	
3ii <i>iso-/n-C₅</i> <i>neo-/n-C₅</i>	$N_{C_5} > 0.7$ mol/kg $S_{iso-/n-C_5} > 3$ $S_{neo-/n-C_5} > 4$	TACPAP	6.19	0.77 ± 0.23	0.332 ± 0.323 [3.00 ± 2.92]	0.201 ± 0.182 [4.98 ± 4.51]		
4	<i>neo-/n-C₅</i> <i>neo-/iso-C₅</i>	$N_{C_5} > 0.9$ mol/kg $S_{neo-/n-C_5} > 15$ $S_{neo-/iso-C_5} > 2$	QUPJAN	5.93	0.95 ± 0.12		0.063 ± 0.050 [15.93 ± 12.68]	0.465 ± 0.078 [2.15 ± 0.36]
5	<i>iso-/n-C₅</i> <i>iso-/neo-C₅</i>	$N_{C_5} > 0.7$ mol/kg $S_{iso-/n-C_5} > 2$ $S_{iso-/neo-C_5} > 25$	DAWBUA	5.53	1.64 ± 0.39	0.28 ± 0.16 [3.57 ± 2.02]		72.38 ± 13.96
			QARCET	5.63	1.21 ± 0.11	0.27 ± 0.04 [3.64 ± 0.58]		29.43 ± 3.79
			HIZQEN	5.11	1.66 ± 0.36	0.47 ± 0.17 [2.12 ± 0.77]		76.67 ± 47.86
			VAPFUP	5.16	0.75 ± 0.18	0.20 ± 0.13 [5.09 ± 3.45]		$(7.04 \pm 1.78) \times 10^3$
			ACOLIP	4.91	1.53 ± 0.36	0.39 ± 0.17 [2.53 ± 1.11]		$(5.95 \pm 5.06) \times 10^3$
			QULLEP	4.90	0.93 ± 0.21	0.26 ± 0.12 [3.86 ± 1.78]		$> 10^6$
6	<i>n-/iso-C₅</i> <i>neo-/iso-C₅</i>	$N_{C_5} > 1.0$ mol/kg $S_{n-/iso-C_5} > 100$ $S_{neo-/iso-C_5} > 100$	ODOXEK	5.23	1.04 ± 0.12	189.27 ± 90.40		0.0029 ± 0.0015 [344.80 ± 173.76]

* *a/b*: *a* is preferentially adsorbed. If $S_{a/b} > 10^6$, the capacity of *b* is vanishingly small. **[...]: inverse-shape selectivity in blue.

5. Adsorption capacity and selectivity *versus* ϕ , LCD and VSA

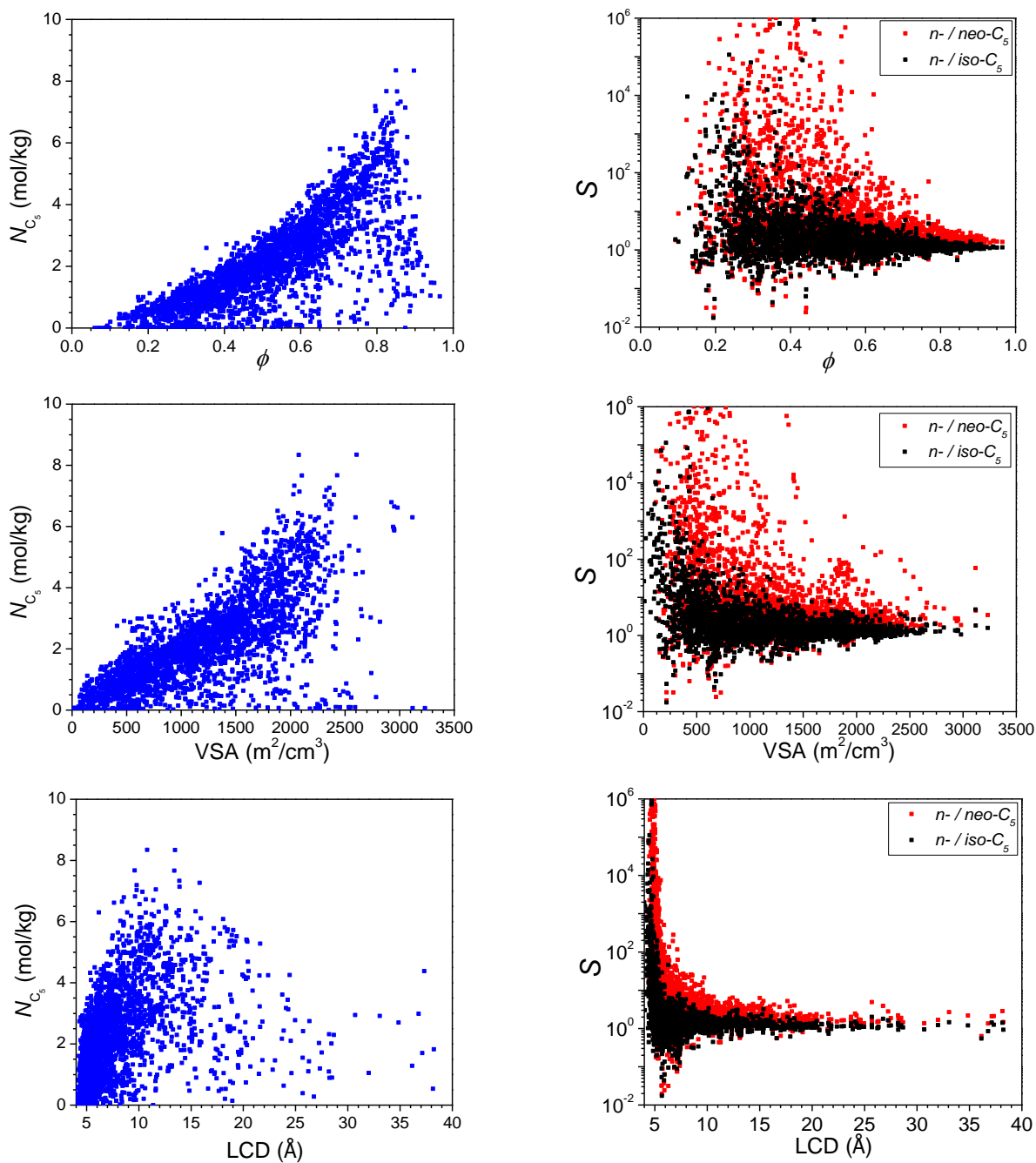


Fig. S2 Adsorption capacity and selectivity *versus* ϕ , VSA and LCD.

6. Pore size distribution between d_1 and d_2

The pore size distribution (PSD) between d_1 and d_2 is defined as²

$$\text{PSD}\%_{(d_1 \sim d_2)} = A_{12} / A_{\text{total}} \times 100\%$$

where A_{total} is the area under the entire PSD curve and A_{12} is the area between d_1 and d_2 .

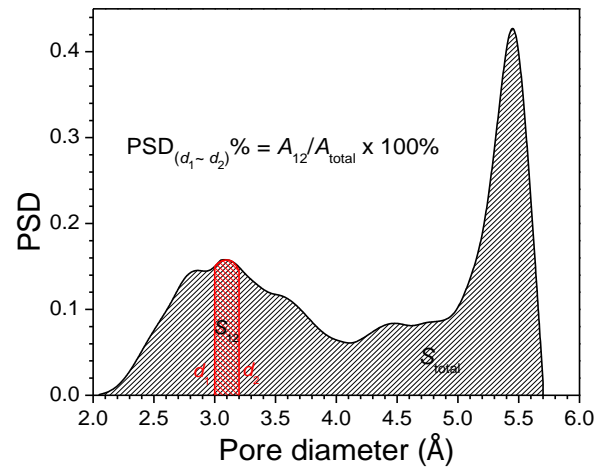
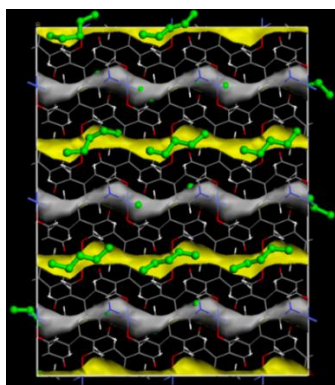
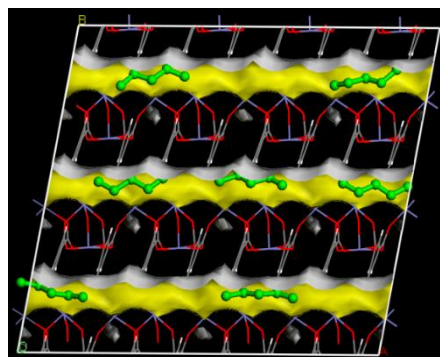


Fig. S3 Pore size distribution between d_1 and d_2 .

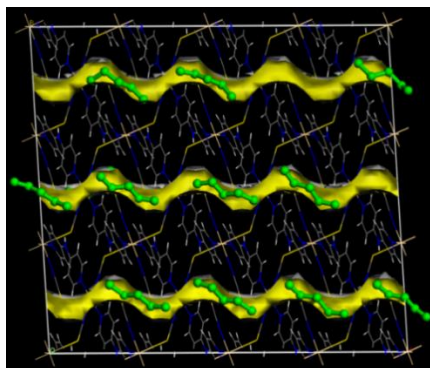
7. Simulation snapshots for different separation mechanisms



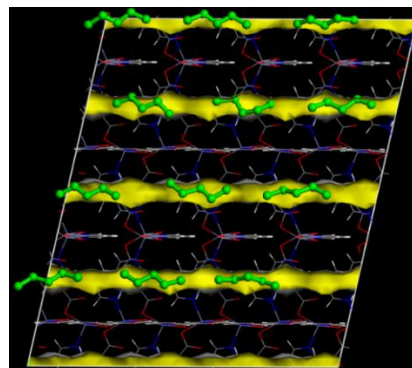
ADIQEL



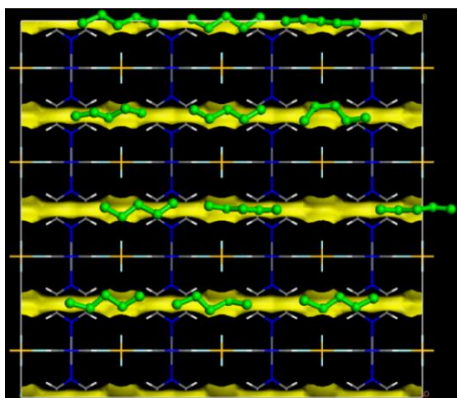
WUCRUH



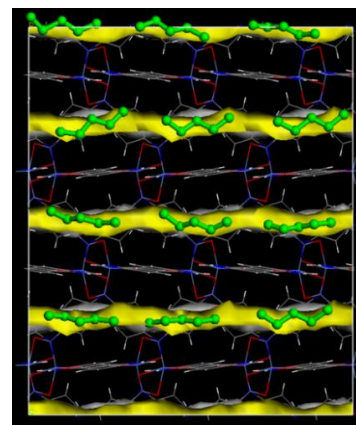
HEXNII



MIMVEJ

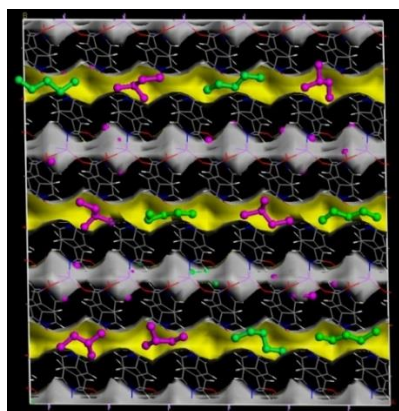


FUDQIF

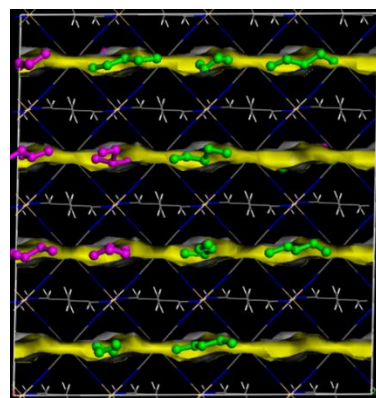


PARMIG

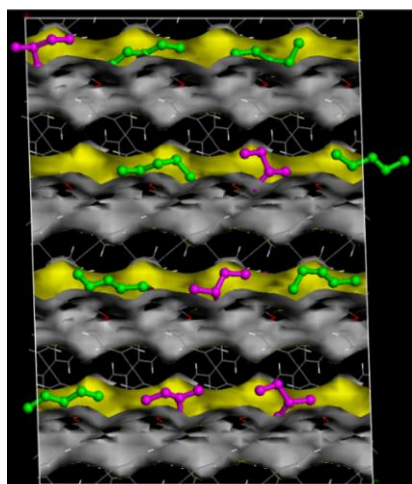
Fig. S4.1 Simulation snapshots for the separation of *n*-/*iso*-C₅, *n*-/*neo*-C₅.



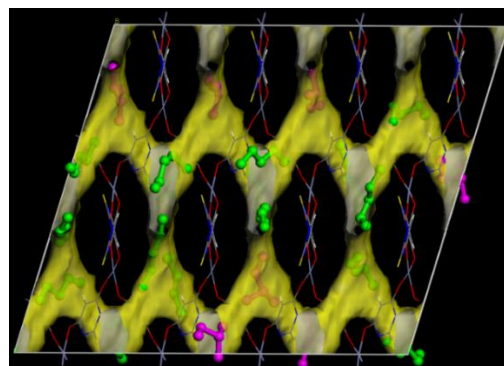
XUNGOD



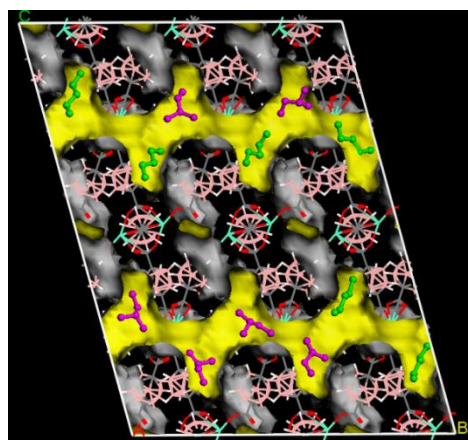
GIFKAH



AFITEP

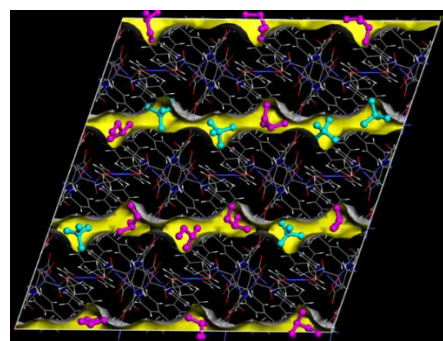


GOGWAB

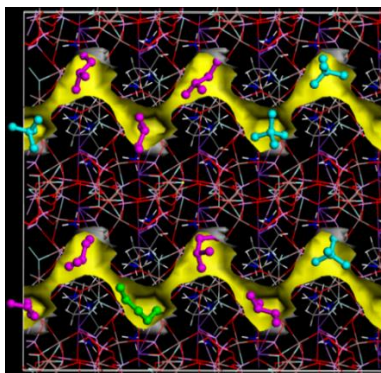


WAZQIZ

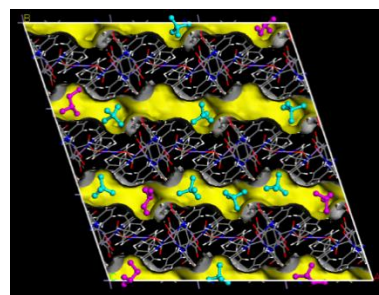
Fig. S4.2 Simulation snapshots for the separation of *n*-/*neo*-C₅, *iso*-/*neo*-C₅.



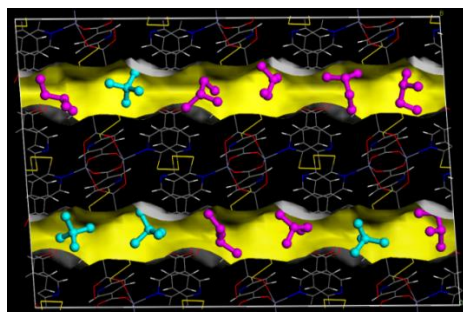
INAMUG



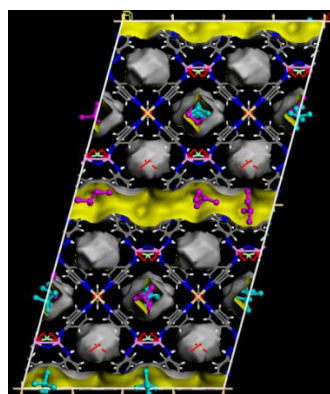
XUVGUQ



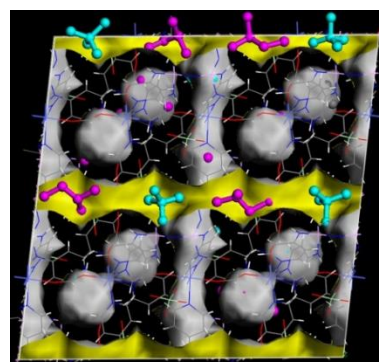
MAJHUC



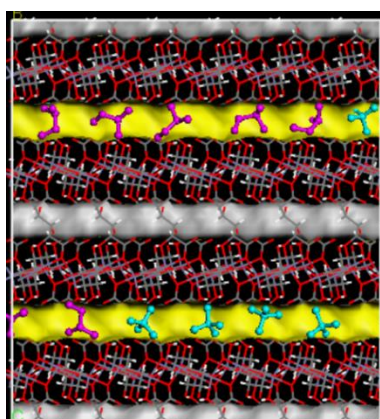
OVICUS



SEMFIB

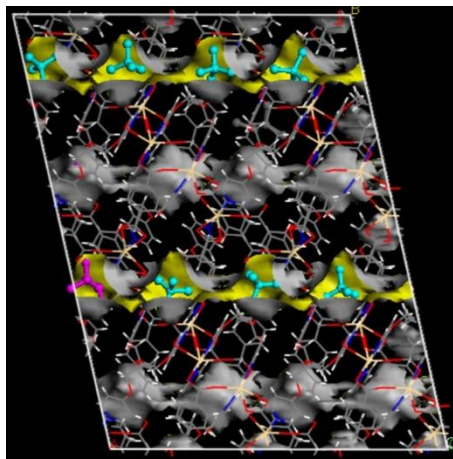


SEMFEX



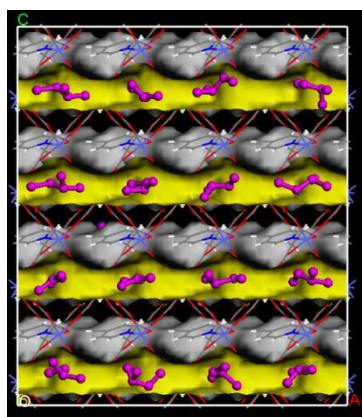
TACPAP

Fig. S4.3 Simulation snapshots for the separation of *iso*-/*n*-C₅, *neo*-/*n*-C₅.

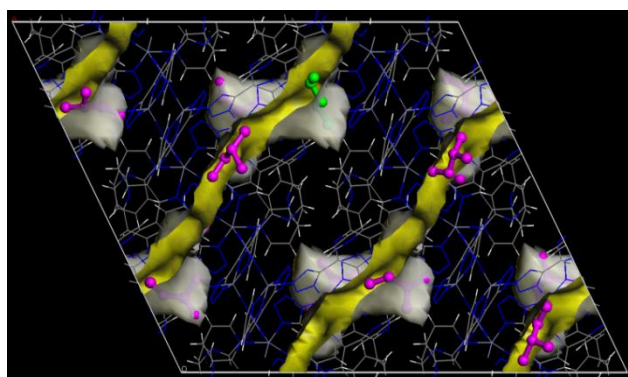


QUPJAN

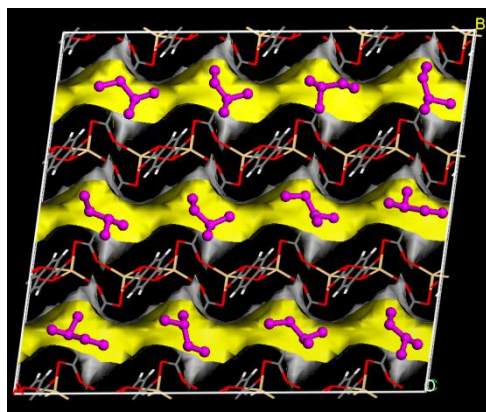
Fig. S4.4 Simulation snapshot for the separation of *neo*-/*n*-C₅, *neo*-/*iso*-C₅.



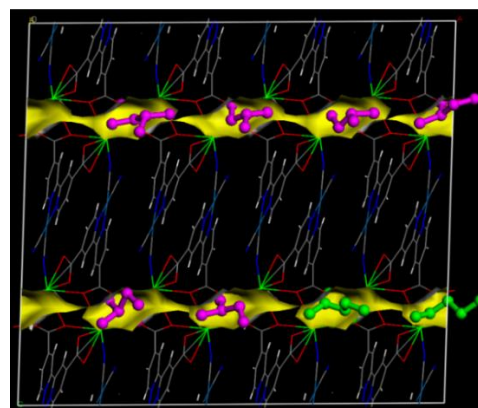
DAWBUA



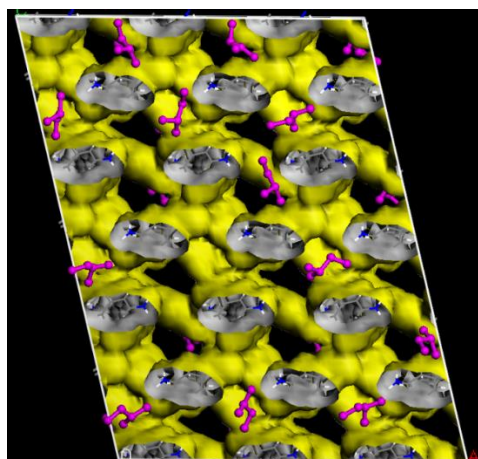
QARCET



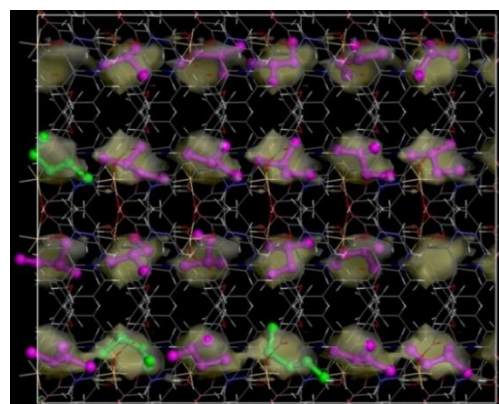
HIZQEN



VAPFUP



ACOLIP



QULLEP

Fig. S4.5 Simulation snapshots for the separation of *iso*-/*n*-C₅, *iso*-/*neo*-C₅.

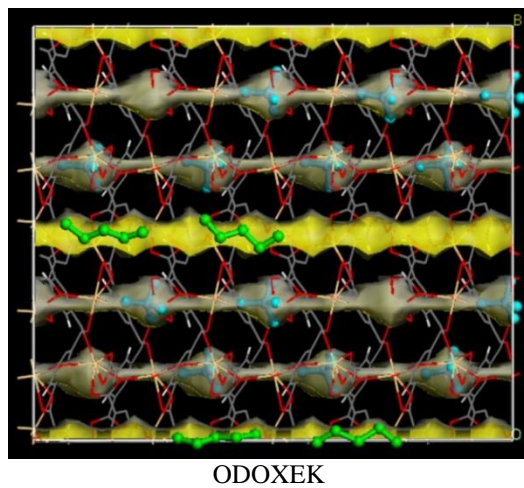


Fig. S4.6 Simulation snapshot for the separation of *n*-*iso*-C₅, *neo*-*iso*-C₅.

8. Molecular models

Table S5 Lennard-Jones parameters of CoRE-MOFs.³

Atom	ϵ/k_B [K]	σ [Å]	Atom	ϵ/k_B [K]	σ [Å]	Atom	ϵ/k_B [K]	σ [Å]
Ac	16.60	3.10	Ge	190.69	3.81	Po	163.52	4.20
Ag	18.11	2.80	Gd	4.53	3.00	Pr	5.03	3.21
Al	254.09	4.01	H	22.14	2.57	Pt	40.25	2.45
Am	7.04	3.01	Hf	36.23	2.80	Pu	8.05	3.05
Ar	93.08	3.45	Hg	193.71	2.41	Ra	203.27	3.28
As	155.47	3.77	Ho	3.52	3.04	Rb	20.13	3.67
At	142.89	4.23	I	170.57	4.01	Re	33.21	2.63
Au	19.62	2.93	In	301.39	3.98	Rh	26.67	2.61
B	90.57	3.64	Ir	36.73	2.53	Rn	124.78	4.25
Ba	183.15	3.30	K	17.61	3.40	Ru	28.18	2.64
Be	42.77	2.45	Kr	110.69	3.69	S	137.86	3.59
Bi	260.63	3.89	La	8.55	3.14	Sb	225.91	3.94
Bk	6.54	2.97	Li	12.58	2.18	Sc	9.56	2.94
Br	126.29	3.73	Lu	20.63	3.24	Se	146.42	3.75
C	52.83	3.43	Lr	5.53	2.88	Si	202.27	3.83
Ca	119.75	3.03	Md	5.53	2.92	Sm	4.03	3.14
Cd	114.72	2.54	Mg	55.85	2.69	Sn	285.28	3.91
Ce	6.54	3.17	Mn	6.54	2.64	Sr	118.24	3.24
Cf	6.54	2.95	Mo	28.18	2.72	Ta	40.75	2.82
Cl	114.21	3.52	N	34.72	3.26	Tb	3.52	3.07
Cm	6.54	2.96	Na	15.09	2.66	Tc	24.15	2.67
Co	7.04	2.56	Ne	21.13	2.66	Te	200.25	3.98
Cr	7.55	2.69	Nb	29.69	2.82	Th	13.08	3.03
Cu	2.52	3.11	Nd	5.03	3.18	Ti	8.55	2.83
Cs	22.64	4.02	No	5.53	2.89	Tl	342.14	3.87
Dy	3.52	3.05	Ni	7.55	2.52	Tm	3.02	3.01
Eu	4.03	3.11	Np	9.56	3.05	U	11.07	3.02
Er	3.52	3.02	O	30.19	3.12	V	8.05	2.80
Es	6.04	2.94	Os	18.62	2.78	W	33.71	2.73
F	25.16	3.00	P	153.46	3.69	Xe	167.04	3.92
Fe	6.54	2.59	Pa	11.07	3.05	Y	36.23	2.98
Fm	6.04	2.93	Pb	333.59	3.83	Yb	114.72	2.99
Fr	25.16	4.37	Pd	24.15	2.58	Zn	62.39	2.46
Ga	208.81	3.90	Pm	4.53	3.16	Zr	34.72	2.78

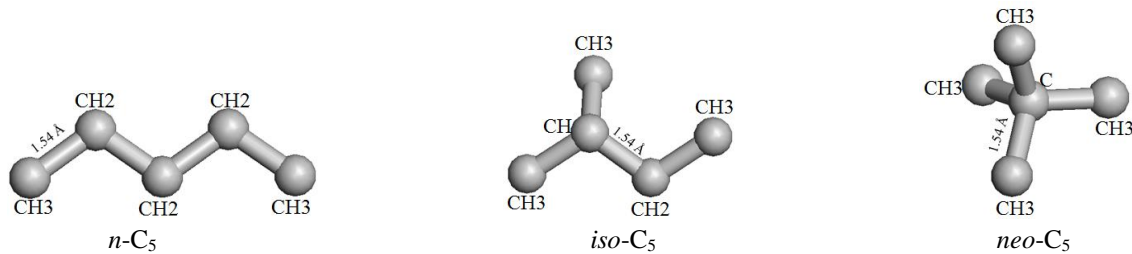


Fig. S5 United-atom model of C_5 isomers.

C_5 isomers (n - C_5 , iso - C_5 and neo - C_5) were represented by a united-atom model with CH_x ($x = 3, 2, 1$ and 0) as a single interaction site (**Fig. S5**). In addition to the nonbonded Lennard-Jones potential, there exist bond bending and torsional potentials,

$$u_{\text{bending}}(\theta) = 0.5k_{\theta}(\theta - \theta^{\circ})^2$$

$$u_{\text{torsion}}(\varphi) = c_0 + c_1[1 + \cos\varphi] + c_2[1 - \cos(2\varphi)] + c_3[1 + \cos(3\varphi)]$$

where θ and φ are the bending and torsional angles, respectively; k_{θ} and c_i are the force constants. These parameters (**Table S6**) were adopted from the transferable potentials for phase equilibria (TraPPE) force field.⁴ The cross interaction parameters between MOFs and C_5 isomers were estimated by the Lorentz-Berthelot combining rules.

Table S6 Lennard-Jones, bond bending and torsional potential parameters.

Atom	ε/k_B (K)	σ (Å)
CH ₃	98.0	3.75
CH ₂	46.0	3.95
CH	10.0	4.68
C	0.5	6.40

	n - C_5		iso - C_5		neo - C_5			
	θ°	k_{θ}/k_B (K/rad ²)	θ°	k_{θ}/k_B (K/rad ²)	θ°	k_{θ}/k_B (K/rad ²)		
CH ₃ -CH ₂ -CH ₂	114.0°	62500	CH ₃ -CH ₂ -CH	114.0°	62500	CH ₃ -C-CH ₃	109.5°	62500
			CH ₃ -CH-CH ₃	112.0°	62500			
			CH ₃ -CH-CH ₃	112.0°	62500			

n - C_5				
	c_0/k_B (K)	c_1/k_B (K)	c_2/k_B (K)	c_3/k_B (K)
CH ₃ -CH ₂ -CH ₂ -CH ₂	0.00	355.03	-68.19	791.32

iso - C_5				
	c_0/k_B (K)	c_1/k_B (K)	c_2/k_B (K)	c_3/k_B (K)
CH ₃ -CH-CH ₂ -CH ₃	-251.06	428.73	-111.85	441.27

Table S7 Adsorption of equimolar C₅ isomer mixture in VICDOC at 433 K and a total pressure of 30 kPa.

	This study	Krishna and van Baten ⁵
N_{n-C_5} (mol/kg)	1.84	1.81
N_{iso-C_5} (mol/kg)	9.5×10^{-2}	6.0×10^{-2}
N_{neo-C_5} (mol/kg)	2.5×10^{-4}	4.4×10^{-4}

References

1. Linstrom, P. J., *NIST Chemistry WebBook*. 2010.
2. Qiao, Z.; Peng, C.; Zhou, J.; Jiang, J. W., High-Throughput Computational Screening of 137953 Metal-Organic Frameworks for Membrane Separation of a CO₂/N₂/CH₄ Mixture. *J. Mater. Chem. A* 2016, 4, 15904-15912.
3. Rappe, A. K.; Casewit, C. J.; Colwell, K. S.; Goddard, W. A.; Skiff, W. M., UFF: A Full Periodic Table Force Field for Molecular Mechanics and Molecular Dynamics Simulations. *J. Am. Chem. Soc.* 1992, 114, 10024-10035.
4. Martin, M. G.; Siepmann, J. I., Transferable Potentials for Phase Equilibria. 1. United-Atom Description of *n*-Alkanes. *J. Phys. Chem. B* 1998, 102, 2569-2577.
5. Krishna, R.; van Baten, J. M., Screening Metal-Organic Frameworks for Separation of Pentane Isomers. *Phys. Chem. Chem. Phys.* 2017, 19, 8380-8387.